

## High performance epoxy resin nanocomposites containing both organic montmorillonite and castor oil-polyurethane

Jinbo Li (✉)

Department of Science and Technology, Xi'an Shiyou University, Xi'an 710065, China  
School of Material Science and Engineering, Xi'an Jiaotong University, Xi'an 710049, China  
E-mail: [Lijinbo6036@163.com](mailto:Lijinbo6036@163.com), Fax: +86-29-82663453

Received: 12 November 2005 / Revised version: 15 December 2005 / Accepted: 15 December 2005  
Published online: 9 January 2006 – © Springer-Verlag 2006

### Summary

Epoxy resin/polyurethane interpenetrating polymer network nanocomposites with various contents of organophilic montmorillonite (oM-EP/PU nanocomposites) were prepared by a sequential polymeric technique and an *in situ* intercalation method. X-ray diffraction(XRD), and transmission electronic microscopy(TEM) analysis showed that organophilic montmorillonite (oMMT) disperses uniformly in epoxy resin/ polyurethane interpenetrating networks(IPNs), and the intercalated or exfoliated microstructures of oMMT are formed. Differential scanning calorimetry(DSC) test proved that oMMT promotes the compatibility of EP phase and PU phase, and glass transition temperature( $T_g$ ) of oM-EP/PU nanocomposites improves with increasing oMMT content. Mechanical properties tests and thermal gravity analysis (TGA) indicated that oMMT and the IPNs of EP and PU exhibit synergistic effect on improving mechanical and thermal properties of pure EP. The mechanism of toughening and reinforcing of oM-EP/PU nanocomposites was further discussed by scanning electronic microscope(SEM).

### Introduction

Epoxy resin(EP), as one of thermosetting polymers, exhibits an attractive performance of stiffness, strength, thermal stability and creep resistance, and it is widely applied as matrix of coatings, adhesives, and composites. However, because of its highly-crosslinking density, EP has low toughness and poor crack resistance at room temperature. This is the basic reason why a large body of literature has been on the subject of toughening of EP. Major investigations focused on forming blends by adding thermoplastic polymers or rubbers into epoxy resin in order to improve toughness of EP<sup>[1-7]</sup>. For example, epoxy resin is often modified by being dissolved in a small proportion of a liquid rubber, such as amine-terminated butadiene acrylonitrile copolymer(ATBN)<sup>[4,5]</sup> and carboxy-terminated acrylonitrile copolymer(CTBN)<sup>[6,7]</sup>. Interpenetrating polymer networks (IPNs) has been used to describe the combination of crosslinked polymer networks in which at least one polymer is synthesized or crosslinked in the immediate presence of the other. The mechanical properties of polymer materials with an IPN structure are superior to those of ordinarily polymers. Recently, interpenetrating polymer networks (IPNs) using a rubbery polyurethane

(PU) phase have been considered for improving toughness of EP<sup>[8-11]</sup>. It reveals that the presence of intermolecular hydrogen bonding between the hydroxyl group in EP and the isocyanate group in PU exerts an important role in increasing good network interlocking in the IPN formation<sup>[8]</sup>. Although IPNs of polyurethane and epoxy resin are very efficient for improving the fracture properties of epoxy resin, strength and thermal properties of the IPNs are often lower than pure EP<sup>[12,13]</sup>.

As is well-known, addition of some inorganic nanoparticles, such as layered clay<sup>[14-17]</sup>, carbon nanotubes<sup>[18-20]</sup> or spherical silica<sup>[21, 22]</sup>, into EP matrix is an effective method to improve the strength of EP. To avoid deterioration in the inherent stiffness and strength and a reduction in the thermal stability of EP IPNs, adding nanoparticles may be an effective approach. However, the hybrid approach of adding both nanofillers and rubbers into epoxy resin is limited. More recently, Liu et al. prepared hybrid epoxy nanocomposites modified with carboxyl-terminated butadiene acrylonitrile rubber and organoclay<sup>[23]</sup>. Zhang et al. found that adding nanosilica to interpenetrating polymer networks (IPN)s of polyurethane and epoxy resin improved the properties of compatibility, damping and phase structure of the IPN matrices<sup>[24]</sup>. Jia et al. prepared PU nanocomposites containing EP and oMMT, and the results proved that the PU nanocomposites exhibited excellent mechanical properties and high water resistance<sup>[25]</sup>. The major concern of this paper is to study the preparation of the EP/PU IPNs nanocomposites containing oMMT, and synergistic effects of oMMT and EP/PU IPNs on improving mechanical and thermal properties of pure EP were investigated by XRD, TEM, SEM, TGA, DSC, and mechanical test. The results obtained in this paper will be helpful for the optimization of EP.

## Experimental

### *Materials*

2,4-toluene diisocyanate(TDI) and hexadecyl trimethyl ammonium bromide were made in Shanghai Chemical Reagent Co(China). Commercial castor oil, diglycidyl ether of biphenol A (DGEBA) and 2,4,6-tri(dimethylaminomethyl) phenol(DMP-30) were made in Tianjin Chemical Co(China). The montmorillonite was obtained by purification of natural sodium bentonite, provided by South Clay Co(China). The method for preparing oMMT was similar to Kawasumi *et al.*'s<sup>[26]</sup>. Castor oil and DGEBA were dried under a vacuum condition prior to use.

### *Synthesis of EP/PU IPNs*

A typical synthesis method was as follows: a weighed amount of castor oil was placed in a round-bottomed flask, heated until 60 °C, and thoroughly mixed with a predetermined amount of TDI, the reaction system was stirred vigorously with a Teflon-coated magnetic stir bar, under a dry nitrogen atmosphere, for about 45 min to form an urethane prepolymer. Then, quantitative epoxy precursor was added to the system which was stirred for a while before adding 1.5%, by weight, of DMP-30 (based on the amount of DGEBA).The mixture was degassed under a vacuum for some minutes and then poured and pressed into the preheated Teflon molds. The filled molds were heated until 120 °C and then the IPNs samples were cured at that temperature for some hours to perform the completion of the polymerization in both phases<sup>[27]</sup>.

### *Synthesis of oM-EP/PU nanocomposites*

The epoxy precursor and different amounts of oMMT (1%, 3%, 5%, by weight, based on the amount of the epoxy precursor) were placed in a round-bottomed flask, heated until 80 °C and stirred vigorously for about 8 h, then the PU prepolymer were added into the epoxy precursors containing oMMT. The following steps were the same as synthesis of EP/PU IPNs. The EP/PU IPNs nanocomposites with different oMMT content were prepared, marked as EP/PU1, EP/PU3 and EP/PU5, respectively. In these nanocomposites, the weight ratio of PU and EP is 25:75.

### *Characterization*

Wide-angle X-ray diffraction(WAXD) was used to determine the basal spacings in the nanocomposites, and the test was performed at room temperature with a Rigaku X-Ray diffractometer(Japan) with a  $\text{CuK}\alpha$  radiation source( $\lambda=0.154$  nm), which was operated at 40 kV and 30 mA. The phase microstructure of the nanocomposites was observed by a JSM-35C scanning electron microscope(JEOL CO. Japan) operated at 20 kV. TEM observations were carried out on a H-600 electron microscope (Hitachi CO. Japan) with an acceleration voltage of 120 kV. Samples were prepared by a LKB Bromma 2088 Ultratome at room temperature. Tensile tests were done using a PDL series instron tensile strength tester at a crosshead speed of 5 mm/min at 20 °C, The measurements were performed according to the Chinese standard GB/T 528-1998. The critical stress intensity factor ( $K_{IC}$ ) was measured in the three-point bending mode following ASTM standard E399. Specimens were polished to 10.00 × 4.00 × 80.0 mm bars. The span of the two support beams was 60.0 mm and a 0.5 mm notch was made in the sample using a hacksaw. The critical stress intensity factor was calculated from the following equations:

$$K_{IC}=Y\sigma_0a^{1/2}; \sigma_0=3SP_b/2Bw^2 \quad (1)$$

$$Y=1.93-3.07(a/w)+14.53(a/w)^2-25.11(a/w)^3+25.80(a/w)^4 \quad (2)$$

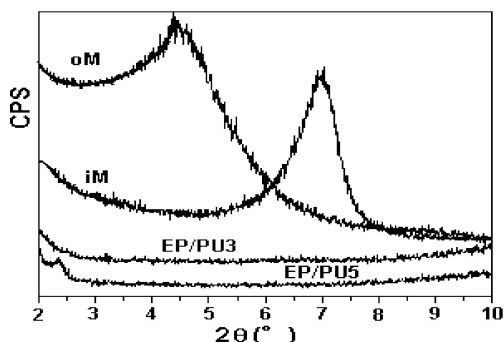
where  $P_b$  is the load at fracture,  $B$  is the sample thickness,  $w$  is the sample width,  $S$  is the length of span, and  $a$  is the crack length.

Differential scanning calorimetry (DSC) tests were carried out on the DSC 822° (METTLER TOLEDO) to measure the glass transition temperature( $T_g$ ). Temperature and energy calibration were carried out with indium. The scan rate was 10 °C /min within the temperature range of -50~150 °C. The  $T_g$  is taken at the median point in the range of glass transition. TGA thermograms were obtained on a Q600 STD Instruments equipment(TA CO. Unite States), under a nitrogen atmosphere at a heating rate 10 °C /min, and scanned from room temperature to 600 °C, The samples ranged between 15 mg and 25 mg in weight and were placed in platinum sample pans under a continuous nitrogen flow 100 mL/min.

## **Results and discussion**

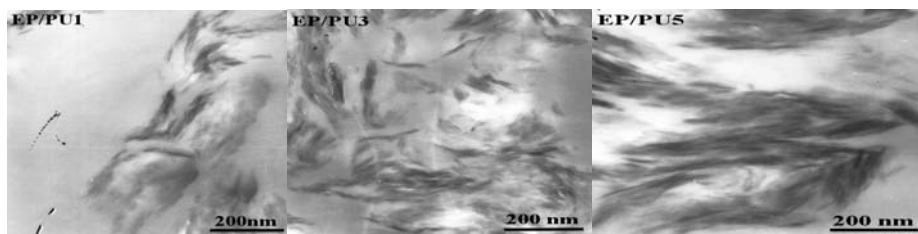
### *XRD and TEM analysis*

Figure 1 exhibits the XRD plots of the MMT before and after treatment and oM-EP/PU nanocomposites with different content of oMMT. Their d-spacings are calculated using Bragg's relation according to the angle of the 001 diffraction peak in the XRD pattern.



**Figure 1.** XRD plots of the different materials.

It can be seen from Figure 1 that after treatment, the diffraction peak of MMT shifts from  $6.9^\circ$  to  $4.5^\circ$ , corresponded to an increase of the  $d_{001}$ -spacing from 1.27 nm of pristine MMT to 1.96 nm of treated MMT, which means hexadecyl trimethyl ammonium cations effectively expand the d-spacings of MMT. When 3% oMMT was added to the EP/PU matrix, the XRD plot of EP/PU3 shows no obvious diffraction peaks from  $2.0$  to  $10.0^\circ$ , which means that an exfoliated structure is derived. But, a relatively small diffraction peak displays at  $2\theta = 2.3^\circ$  in the WAXD pattern of the EP/PU5, which indicates that most of oMMT in EP/PU5 is aggregate. TEM can further provide more direct information on morphology in real space. As observed by Figure 2, oMMT can disperse uniformly in EP/PU IPNs matrix. But, it is obvious that the degree of clay exfoliation in EP/PU1 or EP/PU3 is higher than that in EP/PU5. These results proved that a complete and effective entry of monomers into the oMMT layers is very difficult when oMMT content is higher, which is consistent with the pure EP/oMMT nanocomposites prepared by Chin et al.<sup>[28]</sup> and Kornmann et al.<sup>[14]</sup>.



**Figure 2.** The TEM patterns of the EP/PU IPNs nanocomposites with different oMMT content.

#### *Mechanical properties test and SEM analysis*

The tensile strength, the elongation at break, and  $K_{IC}$  are tested to evaluate the strength and the toughness of pure epoxy and its composites, respectively. The results are shown in Table 1. According to Table 1, addition of PU to EP matrix can remarkably increase elongation at break and fracture toughness of pure EP, but the tensile strength decreases, which indicates that the interpenetrating polymer networks between EP and PU improves toughness of pure EP. While addition of oMMT to EP/PU IPNs, the tensile strength increases with increasing oMMT content, and the fracture toughness improves a little bit, which indicates that oMMT, acted as a reinforcing filler, remedies

**Table 1** Thermal properties of oM-EP/PU nanocomposites.

Samples	Tensile strength/MPa	Elongation at break/%	$K_{IC}/(\text{MPa}\cdot\text{m}^{1/2})$
Pure EP	57.0	0.5	0.53
EP/PU0	42.8	5.5	1.03
EP/PU1	51.1	6.5	1.17
EP/PU3	68.6	7.0	1.38
EP/PU5	80.2	6.0	1.19

the decrease of tensile strength of EP/PU IPNs. These results prove that oMMT and EP/PU IPNs exhibit synergistic effect on improving strength and toughness of pure EP. It is believed that the outstanding properties of polymer/clay nanocomposites derive from the unique phase morphology and improved interfacial properties<sup>[29]</sup>. SEM patterns of fractured surface of pure EP and its composites are shown in the Figure 3. It is obvious from the Figure 3(a) that fractured surface of pure EP is smooth because there is no obstruction in the path of the crack, which lows the resistance to crack propagation. Figure 3(b) shows rough fractured surface, and presents many cavities(indicated by a black arrow), which suggests that the internal cavitation of the fractured surface followed by plastics shear yielding is probably the prevailing toughening mechanism for EP/PU IPNs. As oMMT is added, oMMT particles disperse uniformly in EP/PU IPNs matrix, and induce many microcracks at the edge of oMMT layers, as shown by a white arrow in Figure 3(c).These microcracks may absorb fractured energies to improve toughness and strength. These observations prove that cavities and micro-cracks are responsible for improving toughness and strength of oM-EP/PU nanocomposites. In addition, it is well known that clay layers in the polymer matrix play the role of reinforcement through stress transfer to the platelet particles.

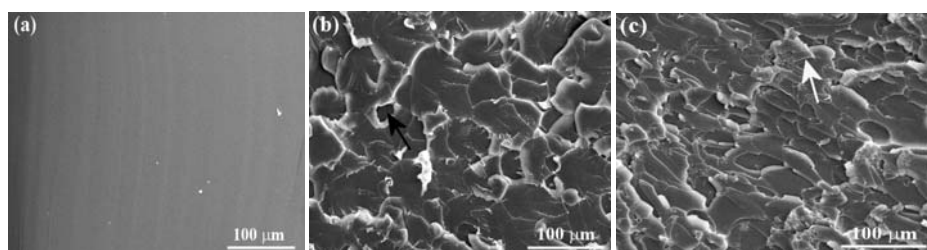


**Figure 3.** SEM patterns of different samples. (a)-Pure EP; (b)-EP/PU IPNs with 25% PU; (c)-EP/PU3.

#### *Thermal properties test*

The glass transitions of oM-EP/PU nanocomposites were measured by DSC and are reported in Figure 4 as a function of the oMMT percent, and the glass transition temperatures( $T_g$ s) are listed in Table 2. The DSC plots for oM-EP/PU nanocomposites with different oMMT contents show two distinct  $T_g$ s, which reveals the phase separation morphology. The lower  $T_g$ ( $T_{g1}$ ) is attributed to the PU-rich phase and the higher  $T_g$ ( $T_{g2}$ ) to the EP-rich phase. With increasing oMMT content, both  $T_{g1}$  and  $T_{g2}$  increase, but the increase of  $T_{g1}$  is faster than that of  $T_{g2}$ , which indicates oMMT has closer relation with PU-rich phase than EP-rich phase. It may be because more

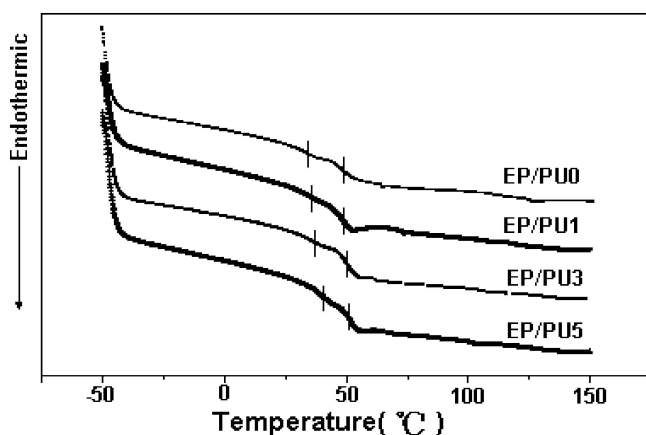


**Figure 4.** DSC curves of oM-EP/PU nanocomposites with different oMMT contents.

hydrogen bonds are formed between PU chain and oMMT. Moreover, these two distinct  $T_g$ s were systematically shifted towards each other with increasing oMMT content, which indicates that the oMMT as a compatibilizer improves the miscibility between EP and PU. Similar phenomena were also observed by Ray et al.<sup>[30]</sup>, Jia et al.<sup>[25]</sup> and Gelfer et al.<sup>[31]</sup> This is one of reasons for explaining the synergistic effect of oMMT and EP/PU IPNs on improving strength and toughness of pure EP.

The thermal stability of EP composites containing PU and oMMT was tested by the thermogravimetric analysis (TGA), and the results are plotted in Figure 5, and the maximal decomposition temperatures ( $T_{max}$ s) of EP composites are listed in Table 2. As shown in Table 2, the  $T_{max}$  of pure EP is about 435.79 °C. With the addition of PU, the  $T_{max}$ s of EP/PU IPNs decrease, which proves that the thermal stability of EP/PU IPNs is lower than that of pure EP. But, adding oMMT into EP/PU IPNs improves thermal stability. It is clear that the  $T_{max}$ s of oM-EP/PU nanocomposites increase with increasing oMMT content, as seen from Figure 5(b). Especially,  $T_{max}$  of EP/PU5 is 4.06 °C higher than that of pure EP, and 18.16 °C higher than that of pure EP/PU IPNs(EP/PU0). The stable morphology of the dispersed phase and the presence of

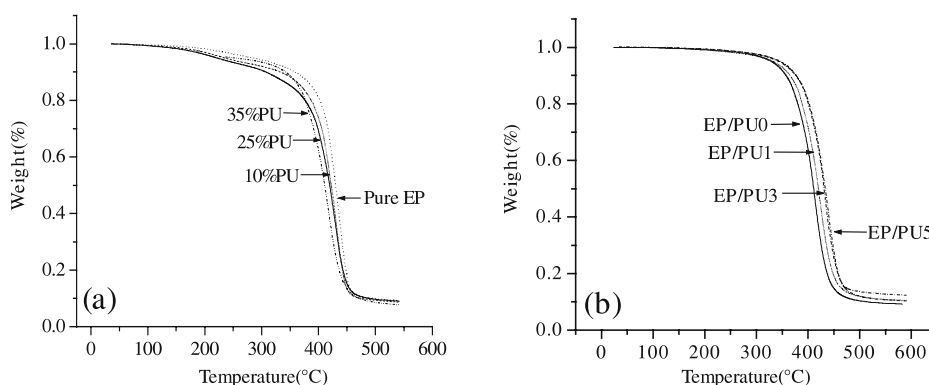


**Figure 5.** TGA curves of EP composites. (a)-TGA curves of pure EP and EP/PU IPNs with different PU contents; (b)-TGA curves of oM-EP/PU nanocomposites with different oMMT contents.

**Table 2** Thermal properties of oM-EP/PU nanocomposites with different oMMT contents.

Samples	$T_{\max}/^{\circ}\text{C}$	$T_{g1}/^{\circ}\text{C}$	$T_{g2}/^{\circ}\text{C}$	$(T_{g2}-T_{g1})/^{\circ}\text{C}$
Pure EP	435.79			
EP+10%PU	426.48			
EP+35%PU	411.21			
EP/PU0	420.69	33.94	48.92	14.98
EP/PU1	425.01	35.60	48.96	14.36
EP/PU3	437.33	37.27	49.76	12.49
EP/PU5	439.85	40.60	50.59	9.99

intercalated silicate layers may be the main reason for the enhanced thermal stability of the oM-EP/PU nanocomposites. Because the higher barrier property of oMMT can slowdown the oxygen diffusion, thus hindering the oxidation procedure. On the other hand, improvement of the miscibility between EP and PU with addition of oMMT is responsible for enhancing thermal stability of the oM-EP/PU nanocomposites.

### Conclusions

It is concluded from this study that the oM-EP/PU nanocomposites were prepared by intercalating oMMT to interpenetrating polymer networks of EP and PU followed by *in situ* polymerization. XRD and TEM analysis showed that intercalated or exfoliated oMMT layers disperse uniformly in EP/PU IPNs, and the oMMT content influences exfoliation degree of oMMT. DSC test proved that oMMT promotes the compatibility of EP phase and PU phase, and  $T_g$  of oM-EP/PU nanocomposites improves with increasing oMMT content. Mechanical properties tests and TGA indicated that oM-EP/PU nanocomposites present higher toughness, strength, and thermal stability, compared with pure EP or pure EP/PU IPNs. The mechanism of toughening and reinforcing of oM-EP/PU nanocomposites is that cavities and microcracks induced by PU phase and oMMT.

*Acknowledgements.* Financial support from Development Program of Changqing Oil Field, China National Petroleum Corporation(CNPC) is acknowledged.

### References

1. Kaji M, Nakahara K, Endo T (1999) *J Appl Polym Sci* 74: 690.
2. Bascom WD, Cottingham RL, Jones RL, Peyser PJ (1975) *J Appl Polym Sci* 19: 2425.
3. Yee AF, Pearson RA (1986) *J Appl Polym Sci* 21: 2475.
4. Chikhi N, Fellahi S, Bakar M (2002) *J Eur Polym* 38: 251.
5. Shin SM, Shin DK, Lee DC (1998) *Polym Bull* 40: 599.
6. Russell B, Chartoff R (2005) *Polymer* 46: 785.
7. Liu YM, Zhang WD, Zhou HW (2005) *Polym Int* 54: 1408.
8. Park SJ, Jin JS (2001) *J Appl Polym Sci* 82: 775.
9. Park SJ, Kang JG, Kwon SH (2004) *J Polym Sci Part B: Polym Phys* 42: 3841.
10. Raymond MP, Bui VT (1998) *J Appl Polym Sci* 70: 1649.
11. Harani H, Fellahi S, Bakar M (1998) *J Appl Polym Sci* 70: 2603.
12. Robert V, Istvan C, Gabor T, Istvan R, Attila I, Andras V (1998) *J Appl Polym Sci* 68: 111.
13. Li Y, Mao S F (1996) *J Polym Sci Part A: Polym Chem* 34: 2371.
14. Kornmann X, Lindberg H, Berglund L A (2001) *Polymer* 42: 4493.

15. Wu DF, Zhou CX, Fan X, Mao DL, Bian Z (2005) *Polym Degrad Stabil* 87: 511.
16. Chen B, Liu J, Chen HB, Wu JS (2004) *Chem Mater* 16: 4864.
17. Ni Y, Zheng SX, Nie KM (2004) *Polymer* 45: 5557.
18. Khabashesku VN, Margrave JL, Barrera EV (2005) *Diam Relat Mater* 14: 859.
19. Zhao D L, Shen ZM (2005) *J Inorg Mater* 20: 608.
20. Barrau S, Demont P, Maraval C, Bernes A, Lacabanne C (2005) *Macromol Rapid Commun* 26: 390.
21. Ochi M, Matsumura T (2005) *J Polym Sci Part B: Polym Phys* 43: 1631.
22. Matejka L, Strachota A, Plestil J, Whelan P, Steinhart M, Slouf M (2004) *Macromolecules* 37: 9449.
23. Liu W P, Hoa SV, Pugh M (2004) *Polym Eng Sci* 44: 1178.
24. Zhang HW, Wang B, Li HT, Jiang Y, Wang JY (2003) *Polym Int* 52: 1493.
25. Jia QM, Zheng M, Chen HX, Shen RJ (2005) *Polym Bull* 54: 65.
26. Kawasumi M, Hasegawa N, Kato M, Usuki A, Okada A (1997) *Macromolecules* 30: 6333.
27. Raymond MP, Bui VT (1998) *J Appl Polym Sci* 70: 1649.
28. Chin IJ, Thurn-Albrecht T, Kim HC, Russell TP, Wang J (2001) *Polymer* 42: 5947.
29. Wu DF, Zhou CX, Xie F, Mao DL, Zhang B (2005) *Polym Degrad Stabil* 87: 511.
30. Suprakas SR, Mosto B (2005) *Macromol Rapid Commun* 26: 1639.
31. Gelfer MY, Song HH, Liu LZ, Hsiao B, Chu B, Rafailovich M, Mayu S, Vladimir Z (2003) *J Polym Sci Part B: Polym Phys* 41: 44.